

Structural Analyses of Metabolites of Phenolic 1-Benzyltetrahydroisoquinolines in Plant Cell Cultures by LC/NMR, LC/MS, and LC/CD

Kinuko Iwasa,^{*,†} Wenhua Cui,[†] Makiko Sugiura,[†] Atsuko Takeuchi,[†] Masataka Moriyasu,[†] and Kazuyoshi Takeda[‡]

Kobe Pharmaceutical University, 4-19-1 Motoyamakita, Higashinada-ku, Kobe-shi 658-8558, Japan, and Ebara Research Co. Ltd. 4-2-1, Honfujisawa, Fujisawa-shi 251-8502, Japan

Received November 28, 2004

The metabolism of the phenolic 1-benzyltetrahydroisoquinoline alkaloids was studied in cell cultures of *Macleaya* and *Corydalis* species. The crude alkaloid fraction obtained from feeding experiments was investigated by application of the combined LC/NMR and LC/APCI-MS (/MS) techniques. Several metabolites were detected, and their structures (**6** and **8–14**) were identified. Bioconversion of the phenolic 1-benzyltetrahydroisoquinoline (**2**) into the pseudoprotoberberine (**8**) was demonstrated for the first time. LC/APCI-MS and LC/CD experiments carried out on a chiral column permitted the deduction of the major enantiomeric form of the chiral metabolites. Thus, the combination of NMR, MS, and CD data permitted the structural elucidation and stereochemical analysis of the metabolites in the extract matrix solution, without isolation and sample purification prior to the coupling experiments.

The bioconversion of isoquinoline alkaloids from Papaveraceae and Fumariaceae plants and their cell cultures have been investigated by us in combination with assays for certain types of biological activity.^{1–5} These studies have resulted in the discovery of numerous metabolites with antimicrobial, antimalarial, anti-HIV, and anticancer activities.^{2–5} Although protoberberine alkaloids differ in the number and position of various oxygen functions on the aromatic rings A and D, the two oxygenation patterns most frequently encountered within this class of alkaloids are at carbons 2,3,9,10 and 2,3,10,11. The former group occurs most commonly, while the latter has been labeled “pseudoprotoberberine” and is not as widespread.⁶ Some 2,3,10,11-oxygenated alkaloids display higher activity in biological tests (e.g., antimalarial activity) than the corresponding 2,3,9,10-substituted analogues.³ The biosynthetic conversion of the 2,3,9,10-oxygenated protoberberines into other alkaloidal types, such as the protopines, benzophenanthridines, rhoeadines, benzindanoazepines, and spirobenzylisoquinolines, has been demonstrated.^{1,7} However, despite its occurrence in some plant species, including *Corydalis* species,⁶ only our earlier study on the biosynthesis of 2,3,10,11-oxygenated protoberberines has been reported.⁸ The applications of LC/NMR to drug metabolism, identification of natural products in crude plant extracts, and the characterization of isomeric mixtures prepared by chemical reactions have been summarized.^{9–11} The application of LC/NMR to biosynthetic studies was previously demonstrated.⁸ The metabolism of 2,3,10,11-oxygenated protoberberines (pseudoprotoberberine) alkaloids was studied in cell cultures of *Corydalis* species.⁸ Without prior isolation, the structures of the metabolites were determined by LC/NMR and LC/MS analyses. Some new alkaloids were identified, and preliminary evidence for the metabolic pathways leading to the formation of these alkaloids was obtained.

This paper describes the structural analysis of the metabolites obtained from the cell cultures of *Macleaya* and *Corydalis* species fed with phenolic 1-benzyltetrahydroiso-

quinolines, which might serve as precursors to pseudoprotoberberines. Metabolites were identified by the complementary techniques of LC/NMR, LC/MS, and LC/CD.

Results and Discussion

The LC/APCI-MS (Figure 1) of the products obtained by the acid-catalyzed ether cleavage of racemic tetrahydropapaverine (**1**) measured with SIM (selected ion monitoring) and TIM (total ion monitoring) in the positive ion mode (LC/APCI-MS I) indicate the presence of several products having one or more phenolic hydroxyl groups besides the starting material. The protonated molecular ions $[M + H]^+$ of each peak were found to be m/z 344 for peak a (**1**), m/z 330 for peaks b–e, m/z 316 for peaks f–j, m/z 302 for peaks k–n, and m/z 288 for peak o from the total ion chromatogram (TIC) of the LC/APCI-MS analysis. Peak a (**1**) displayed the product ions at m/z 192 and 151 (Scheme 1). Peaks b and c showed the product ions at m/z 192 and 137, while peaks d and e displayed ions at m/z 178 and 151 in the LC/MS-MS analysis. The peaks b–e were separated by repeated preparative HPLC, and the structures of the isomers were determined by ¹H NMR and MS analyses. The position of the hydroxyl group was determined by ¹H NMR and MS analyses. The position of the hydroxyl group was confirmed by NOESY and MS/MS data. The four phenolic 1-benzyltetrahydroisoquinolines, **2**, **3**, **4**, and **5**, corresponding to peaks b–e, were used as precursors. The structures of peaks f–o will be presented elsewhere.

Callus tissues of *M. cordata*, *C. platycarpa* Makino, and *C. ochotensis* var. *raddeana* were incubated at 25 °C on an agar medium containing the substrate (Table 1). Following incubation, media and cells were separated and extracted according to the procedure shown in Figure 2. The alkaloid fractions, E-1, E-2, C-1, and C-2 (Figure 2), were subjected to LC/NMR, LC/MS, and LC/CD.

The LC/NMR spectra were measured in the stopped-flow mode. The LC/APCI-MS(/MS) spectra were measured with Q1 or product ion scan. Molecular weight information was obtained on the basis of a protonated molecular ion $[M + H]^+$ or a product ion recorded in the LC/APCI-MS (/MS). The LC/CD was carried out on a chiral reversed-phase column.

* Corresponding author. Tel: 078-453-0031. Fax: 078-435-2080. E-mail: k-iwasa@kobepharm-u.ac.jp.

[†] Kobe Pharmaceutical University.

[‡] Ebara Research Co. Ltd.

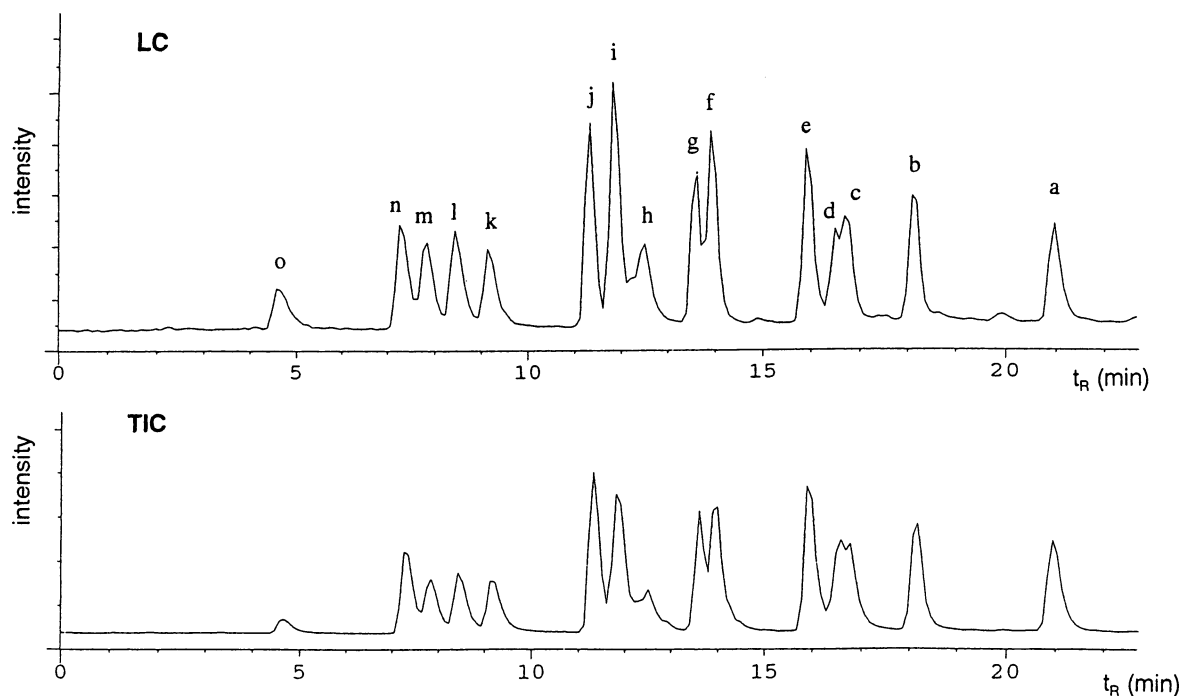
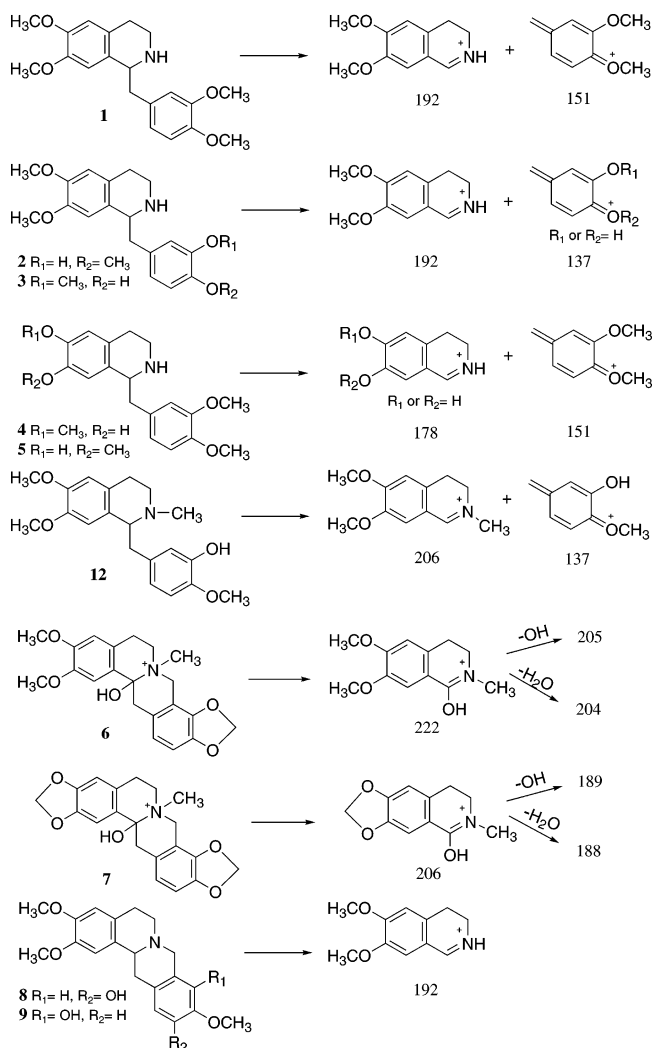


Figure 1. LC/APCI-MS I data of the acid-catalyzed ether cleavage products of tetrahydropapaverine (**1**).

Scheme 1



The precursor **2** was administered to the cultured cells of *M. cordata*, *C. platycarpa*, and *C. ochotensis* var. *rad-*

Table 1. Administration of 1-Benzyltetrahydroisoquinolines (**2**, **3**, **4**, and **5**) to Cultured Cells of *Macleaya* and *Corydalis* Species

no.	callus ^a	substrate (mg)	medium (mL)	wt. of dry cells (g)	incubation period (weeks)	
1	A	2	21	800	7.0	3
2	B	2	50	800	6.6	4
3	C	2	50	800	5.5	4
4	B	3	22	800	5.4	4
5	B	3 and 4	50	800	5.0	4
6	B	5	25	800	4.4	4

^a A: *M. cordata*. B: *C. platycarpa*. C: *C. ochotensis* var. *raddeana*.

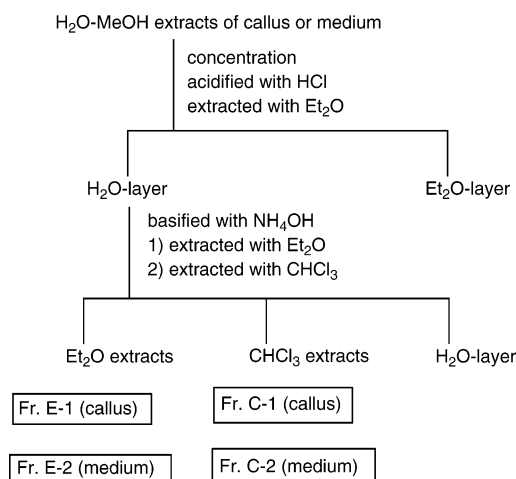


Figure 2. Preparation of samples for LC/NMR, LC/MS, and LC/CD measurements.

deana. Fraction E-2 (Figure 2) obtained from *M. cordata* showed peaks a₁–e₁ in the LC 1 (Figure 3), which displayed the protonated ions $[M + H]^+$ at m/z 370, 354, 342, 342, and 340, respectively, in the LC/APCI-MS. The LC/MS-MS analysis of peak a₁ showed $[M + H]^+$ at m/z 370 and the product ions at m/z 222, 205, and 204. The formation of the product ions is in accord with that of authentic protopine (**7**) (Scheme 1). The stopped-flow ¹H NMR spectrum (A, Figure 4) of peak a₁ displayed four aromatic

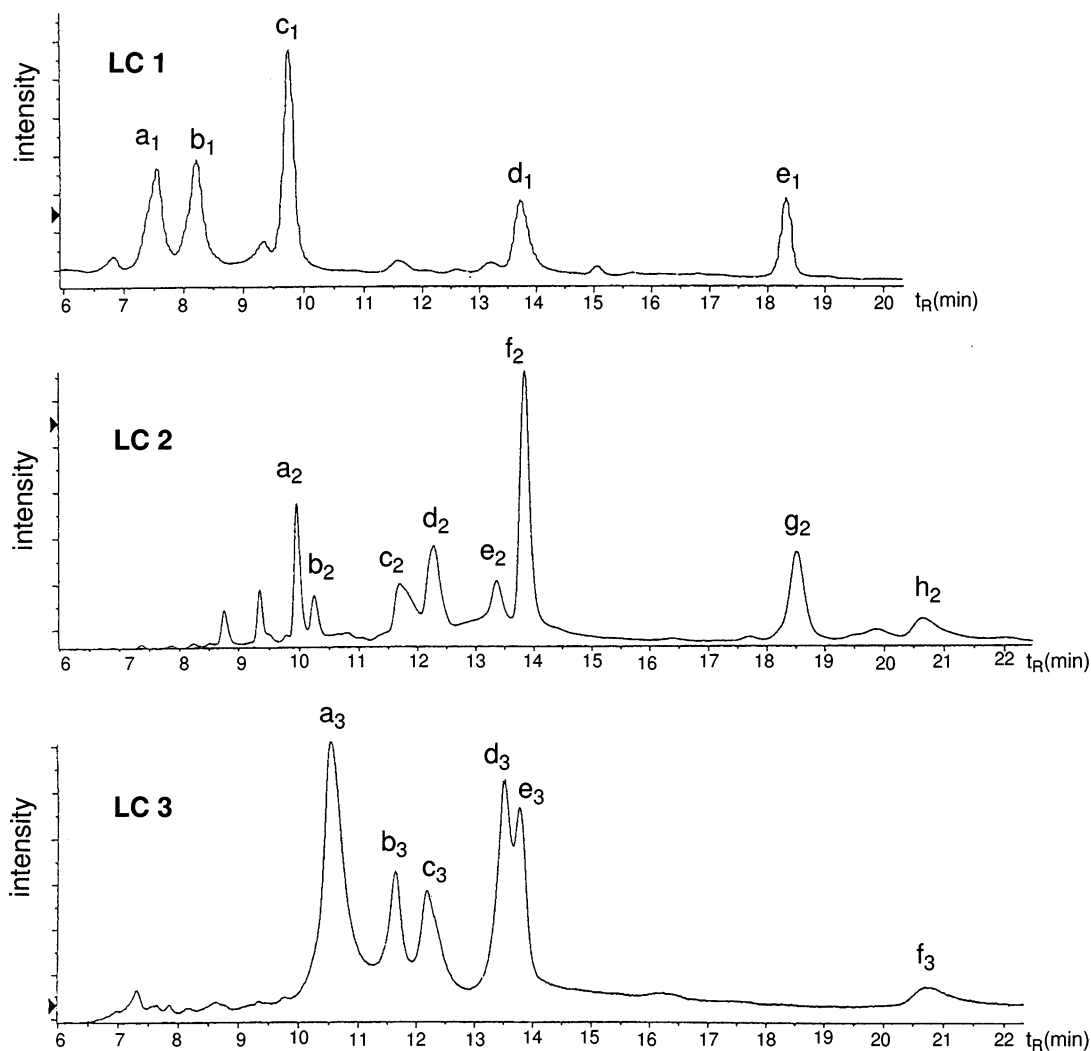


Figure 3. LC data of the alkaloid fraction (E-2) obtained from the feeding of **2** to *M. cordata* (LC 1), *C. platycarpa* (LC 2), and *C. ochotensis* var. *raddeana* (LC 3). Gradient: A 0.1 M NH_4OAc (0.05% TFA)/B CH_3CN (0.05% TFA) LC 1 (A/B: initial 80/20; 25 min 55/45); LCs 2 and 3 (A/B: initial 80/20; 30 min 0/100).

protons at δ 6.85 (3H) and 7.05 (1H), a methylenedioxy group at δ 5.97, two *O*-methyl groups at δ 3.79 (6H), and an *N*-methyl group at δ 2.97. On the basis of this evidence, peak **a**₁ was identified as cryptopine **6**.

Peak **b**₁ in the LC 1 (Figure 3) showed $[\text{M} + \text{H}]^+$ at m/z 354 and the product ions at m/z 206, 189, and 188 in the LC/MS-MS. Its stopped-flow ^1H NMR spectrum exhibited two methylenedioxy groups instead of one and two *O*-methyl groups as observed in peak **a**₁. Peak **b**₁ in LC 1 was identified to be a common component of the callus, propopine **7**.

The LC/MS-MS of peak **c**₁ displayed $[\text{M} + \text{H}]^+$ at m/z 342 and its product ion at m/z 192 (Scheme 1). The stopped-flow ^1H NMR spectrum (B, Figure 4) of peak **c**₁ showed four aromatic protons as singlets at δ 6.84 (H-1), 6.80 (H-4), 6.75 (H-9), and 6.70 (H-12), methylene protons as an AB quartet ($J = 15.0$ Hz) at δ 4.22 and 4.26, and three *O*-methyl groups at δ 3.76 (9H), as well as the other aliphatic protons. These data indicate that the structure represented by peak **c**₁ is corytenchine **8**. The assignments were confirmed by NOESY and by comparison of the stopped-flow ^1H NMR data with those of authentic *S*-corytenchine measured under the same conditions.

The stopped-flow ^1H NMR spectrum (D, Figure 4) of peak **d**₁ in the LC 1 exhibited two aromatic proton singlets at δ 6.86 (H-4) and 6.82 (H-1), two aromatic proton doublets ($J = 8.5$ Hz) at δ 6.93 (H-11) and 6.77 (H-12), three *O*-methyl

groups at δ 3.78 (9H), and nine aliphatic protons in the region between δ 4.3 and 2.9. The LC/MS-MS analysis of peak **d**₁ showed $[\text{M} + \text{H}]^+$ at m/z 342 and its product ion at m/z 192 (Scheme 1). These data identified peak **d**₁ as tetrahydropalmatrubine **9**. Comparison of the stopped-flow ^1H NMR data with those of synthetic **9**, measured under the same conditions, confirmed this identification.

Peak **e**₁ in the LC 1 displayed $[\text{M} + \text{H}]^+$ at m/z 340 and its product ion at m/z 324 in the LC/MS-MS. The stopped-flow ^1H NMR spectrum (F, Figure 4) of peak **e**₁ showed two aromatic proton doublets ($J = 6.0$ Hz) at δ 8.17 and 7.60, an aromatic two-proton AB quartet ($J = 8.0$ Hz) at δ 6.81 and 6.78, three aromatic proton singlets at δ 7.46, 7.28, and 6.93, four *O*-methyl signals at δ 3.91 (3H), 3.85 (3H), and 3.68 (6H), and a methylene singlet at δ 4.48. These data indicated that the structure responsible for peak **e**₁ is papaverine **10**.

A major metabolite in fraction C-2 (Figure 2) obtained from the feeding of **2** to cultured cells of *M. cordata* displayed $[\text{M} + \text{H}]^+$ at m/z 338 and a product ion at m/z 322 in the LC/MS-MS. The stopped-flow ^1H NMR spectrum (see A, Figure 5) of the metabolite showed six aromatic proton singlets at δ 8.70 (H-8), 8.01 (H-13), 7.45 (H-4), 7.27 (H-9), 6.96 (H-1), and 6.90 (H-12), three *O*-methyl groups at δ 3.88 (6H) and 3.83 (3H), and four methylene protons at δ 3.74 (CH_2 -6) and 3.09 (CH_2 -5). These assignments were

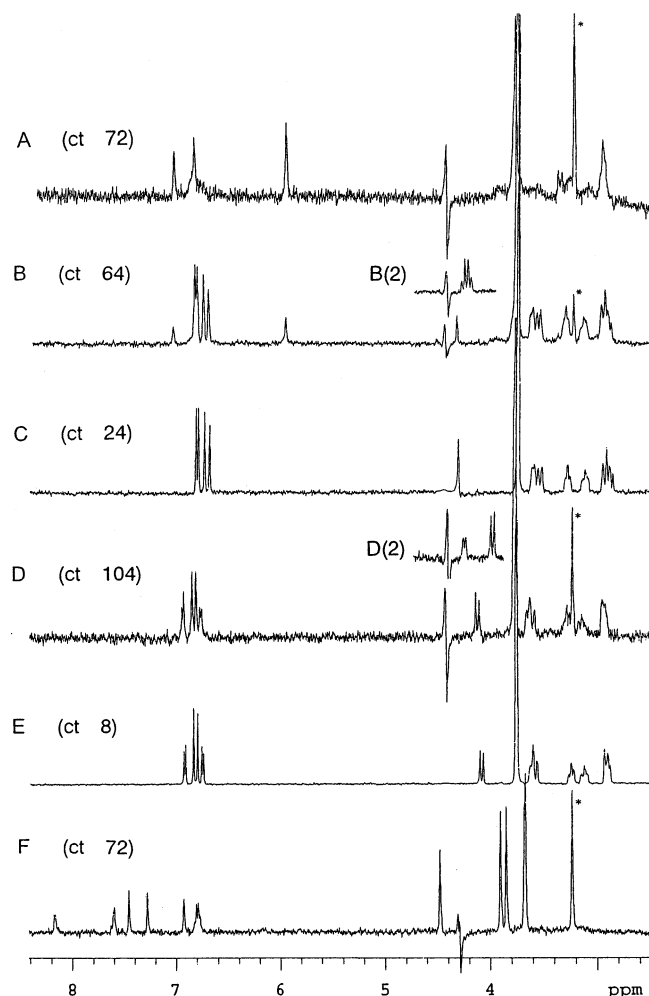


Figure 4. Stopped-flow ^1H NMR spectra of authentic corytenchine (**8**), tetrahydropalmatrubine (**9**), and metabolites (peaks a and c–e in LC 1 of Figure 3) in the alkaloid fraction (E-2) obtained from the feeding of **2** to *M. cordata*. (A) ^1H NMR spectrum of peak a (**6**). (B) ^1H NMR spectrum of peak c (**8**). (B(2)) Use of mobile phases without TFA. (C) ^1H NMR spectrum of authentic **8**. (D) ^1H NMR spectrum of peak d (**9**). (D(2)) Use of mobile phases without TFA. (E) ^1H NMR spectrum of authentic **9**. (F) ^1H NMR spectrum of peak e (**10**). *These signals belong to CH_3OH .

confirmed by NOESY data. The structure of the metabolite was deduced as dehydrocorytenchine **11**.

Fraction E-2 (Figure 2) obtained from feeding of **2** to *C. platycarpa* afforded the peaks a_2 – h_2 in the LC 2 (Figure 3), which displayed $[\text{M} + \text{H}]^+$ at m/z 330, 344, 370, 354, 344, 342, 342, and 342, respectively, in the LC/APCI-MS. From individual LC/NMR and LC/MS-MS data, metabolites associated with peaks c_2 , d_2 , f_2 , and h_2 were deduced to be cryptopine (**6**), protopine (**7**), corytenchine (**8**), and tetrahydropalmatrubine (**9**), respectively. Their data were identical to those of the corresponding metabolites obtained from feeding experiment of **2** to *M. cordata*. The LC/MS-MS of peak a_2 in the LC 2 (Figure 3) showed $[\text{M} + \text{H}]^+$ at m/z 330 and product ions at m/z 192 and 137, while that of peak b_2 displayed $[\text{M} + \text{H}]^+$ at m/z 344 and product ions at m/z 206 and 137 (Scheme 1). From these data, peaks a_2 and b_2 were assumed to be the precursor **2** and its *N*-methyl derivative, laudanine (**12**), respectively. The structures related to peaks e_2 and g_2 are unknown.

Fraction E-2 (Figure 2) obtained from a feeding experiment of **2** to *C. ochotensis* var. *raddeana* showed peaks a_3 – f_3 in the LC 3 (Figure 3), which displayed $[\text{M} + \text{H}]^+$ at m/z 322, 370, 354, 342, 336, and 342, respectively, in the LC/APCI-MS.

Metabolites associated with peaks b_3 , c_3 , d_3 , and f_3 represent cryptopine (**6**), protopine (**7**), corytenchine (**8**), and tetrahydropalmatrubine (**9**), respectively, from their individual LC/NMR and LC/MS-MS data. The LC/MS-MS of peak a_3 in the LC 3 (Figure 3) displayed $[\text{M} + \text{H}]^+$ at m/z 322 and its product ion at m/z 307. The stopped-flow ^1H NMR spectrum (B, Figure 5) of the metabolite displayed four aromatic proton singlets at δ 9.51 (H-8), 8.53 (H-13), 7.47 (H-4), and 6.98 (H-1), two aromatic proton doublets as an AB quartet ($J = 8.5$ Hz) at δ 7.78 (H-11) and 7.74 (H-12), a methylenedioxy resonance at δ 6.34, one *O*-methyl signal at δ 3.86, and four methylene protons at δ 4.74 (CH_2 -6) and 3.15 (CH_2 -5). From these data the structure of the metabolite was deduced to be dehydrocheilanthifoline (**13**). The LC/MS-MS of peak e_3 in the LC 3 (Figure 3) showed $[\text{M} + \text{H}]^+$ at m/z 336 and its product ion at m/z 320. The stopped-flow ^1H NMR spectrum (C, Figure 5) of peak e_3 was similar to that of peak a_3 , but exhibits one more *O*-methyl group than peak a_3 . The structure related to peak e_3 was defined as epiberberine (**14**). According to the LC/NMR (A, Figure 5) and LC/MS-MS data, a main metabolite obtained from fraction C-2 (Figure 2) was identical with dehydrocorytenchine (**11**), which was also found as the metabolite in *M. cordata*.

The precursors, **3**, a mixture of **3** and **4**, and **5** were administered to the cultured cells of *C. platycarpa*. No tetrahydroprotoberberine- or pseudotetrahydroprotoberberine-type alkaloids or their dehydro derivatives were detected in these feeding experiments. However, the corresponding *N*-methyl derivatives of **3**, **4**, and **5** were found by the LC/MS-MS. The *N*-methyl derivatives of **4** and **5** exhibited $[\text{M} + \text{H}]^+$ at m/z 344 and product ions at m/z 192 and 151. The *N*-methyl derivative of **3** displayed $[\text{M} + \text{H}]^+$ at m/z 344 and product ions at m/z 206 and 137 (Scheme 1).

Consequently, although 1-benzyltetrahydroisoquinolines, **3**, **4**, and **5**, were *N*-methylated, in a culture of *C. platycarpa*, they were not bioconverted to any tetrahydroprotoberberine-type alkaloid.

Of the 3'-, 4'-, 7-, and 6-hydroxy isomers (**2**, **3**, **4**, and **5**) of tetraoxygenated 1-benzyltetrahydroisoquinolines having one hydroxyl and three *O*-methyl groups on the aromatic rings A and D, only the 3'-hydroxy isomer **2** was converted into the 2,3,10,11- and 2,3,9,10-oxygenated tetrahydroprotoberberines. This might be due to the substrate specificity of the enzyme which converts the 1-benzyltetrahydroisoquinolines to the tetrahydroprotoberberines. Bioconversion of phenolic 1-benzyltetrahydroisoquinoline (**2**) into pseudotetrahydroprotoberberine (**8**) was demonstrated for the first time. The metabolic transformations in cultured cells of *Macleaya* and *Corydalis* species demonstrated in the present investigations are summarized in Scheme 2.

The applicability of on-line coupling of gradient-eluted, chiral reversed-phase HPLC to the APCI-MS and CD spectroscopy for the stereochemical analysis of the metabolites contained in the crude extracts was also investigated. A detector simultaneously measuring the UV absorbances and the CD effects at constant wavelength in the same detection cell was used for the LC/CD analysis.¹² The *S* absolute configuration at C-13a of tetrahydroprotoberberine alkaloids with levo rotation has been determined by X-ray structure analysis.¹³ Changes in the nature of the substituents in the aromatic rings A and D of the tetrahydroprotoberberines have little or no effect on the specific rotation at the sodium D line.¹⁴ It follows that in general levorotatory tetrahydroprotoberberines have an *S*-configuration. Consequently those that are dextrorotatory correspond to an *R*-configuration.

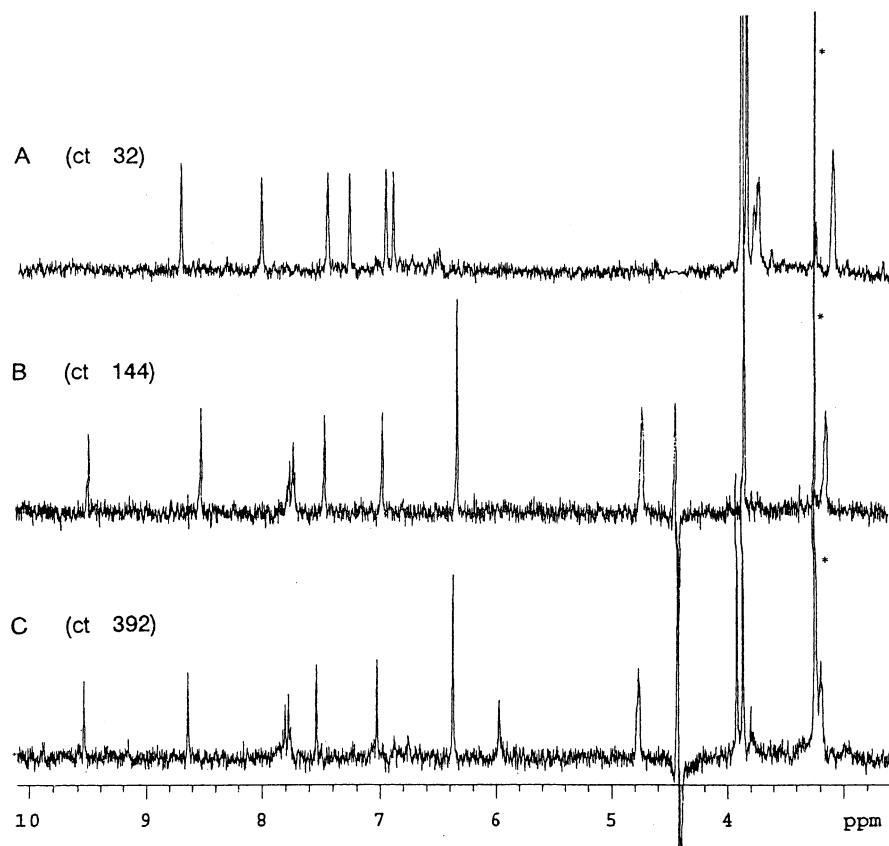


Figure 5. Stopped-flow ^1H NMR spectra of metabolites in the alkaloid fractions (E-2 and C-2) obtained from the feeding of **2** to *C. ochotensis* var. *raddeana*. (A) ^1H NMR spectrum of major peak (**11**) of fraction C-2. (B) ^1H NMR spectrum of peak a (**13**) in the LC 3 (Figure 3) of fraction E-2. (C) ^1H NMR spectrum of peak e (**14**) in the LC 3 (Figure 3) of fraction E-2. *These signals belong to CH_3OH .

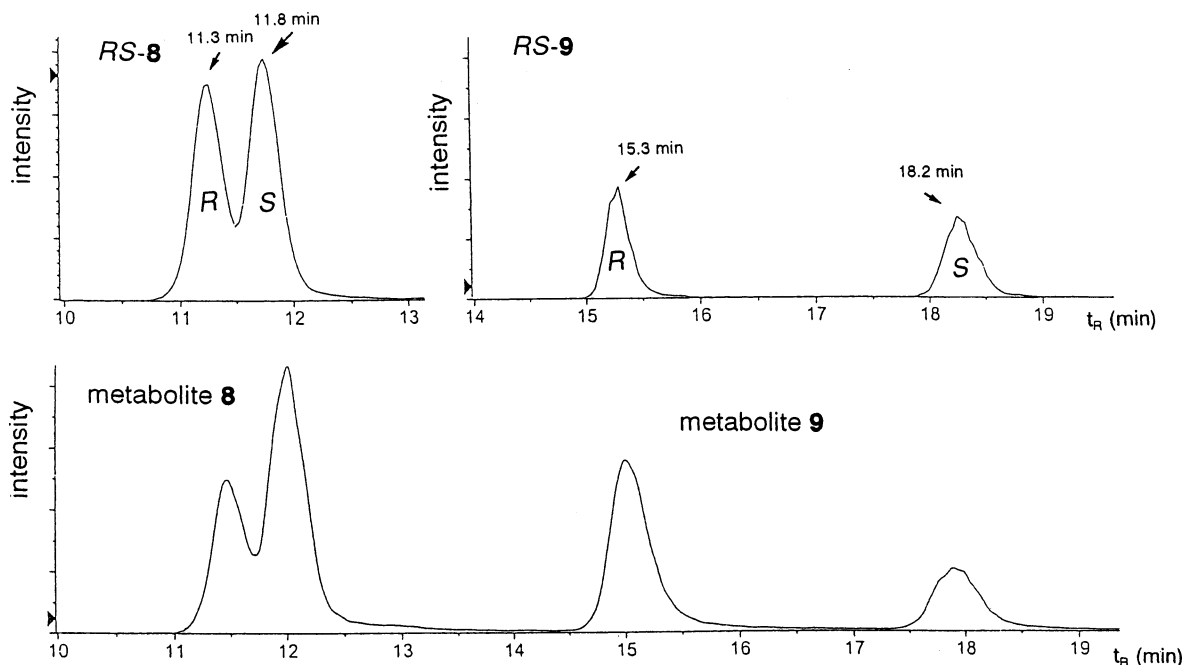


Figure 6. Mass chromatogram of the selected ion m/z 342 in the LC/APCI-MS of *RS*-corytenchine (**8**) and *RS*-tetrahydropalmatrubine (**9**) and in the alkaloid fraction (E-2) obtained from the feeding of **2** to *M. cordata*.

The LC/APCI-MS of synthetic corytenchine (**8**) and tetrahydropalmatrubine (**9**) were measured by chiral chromatography. The protonated molecular ions $[\text{M} + \text{H}]^+$ with m/z 342 for the regioisomers **8** and **9** were selected and reconstructed (Figure 6). The MS chromatograms at 11.3 and 11.8 min were attributed to the enantiomers with the *R*- and *S*-configurations at C-13a of **8**, respectively, which were derived by comparison with the MS chromatogram

of enantiomerically pure natural reference **8** with levo rotation (*S*-configuration).

The MS chromatograms at 15.3 and 18.2 min were assigned as enantiomers with the *R*- and *S*-configurations at C-13a of **9**, respectively. The configuration at C-13a of **9** was determined by the optical rotation of each enantiomer separated by preparative HPLC on a chiral column. From the MS chromatograms (Figure 6) of the selected ions (m/z

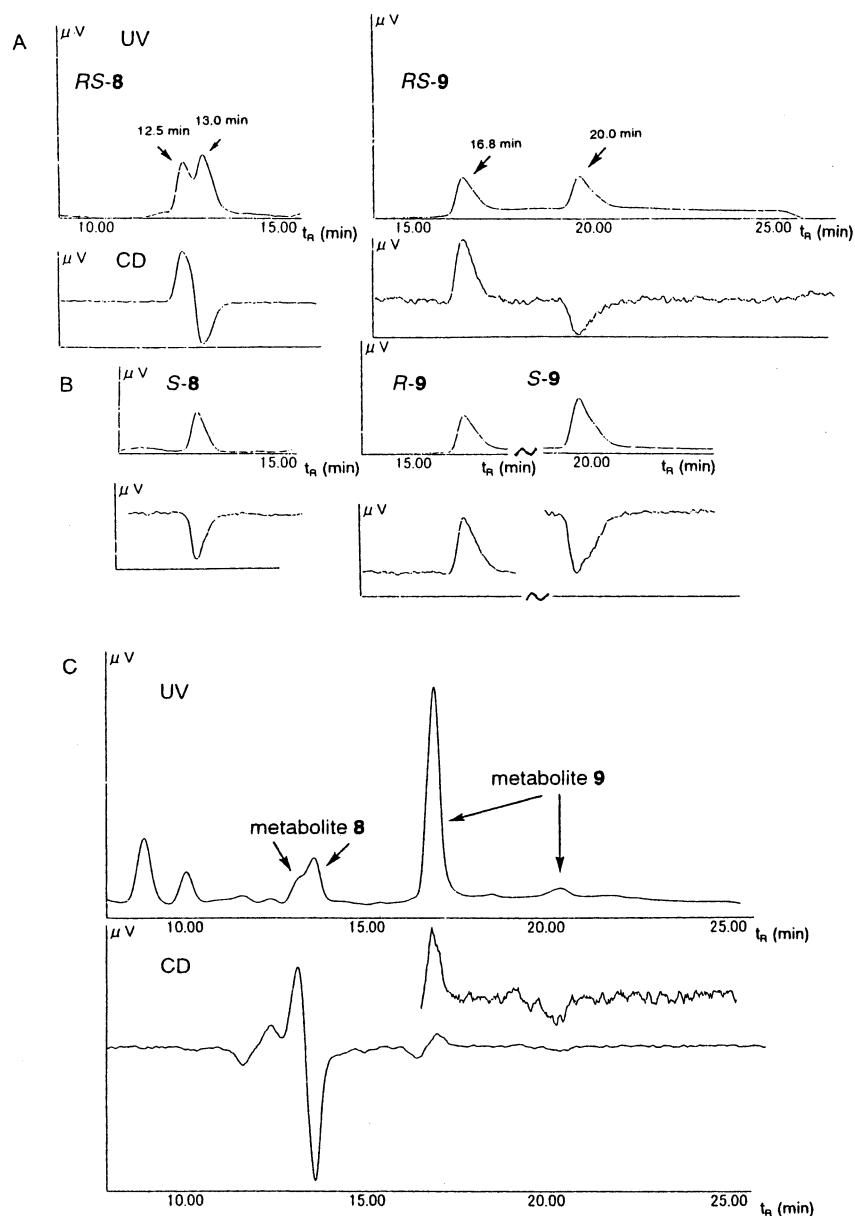


Figure 7. UV and CD chromatograms from the LC/CD of corytenchicine (**8**), tetrahydropalmatrubine (**9**), and their *R*- or *S*-enantiomers, and the alkaloid fraction (E-2) obtained from feeding of **2** to *M. cordata*. (A) UV and CD chromatograms of *RS*-**8** and *RS*-**9**. (B) UV and CD chromatograms of the *R*- or *S*-enantiomer of **8** and **9**. (C) UV and CD chromatograms of the alkaloid fraction (E-2).

Table 2. Composition (%) of the Enantiomers of Corytenchicine (**8**) and Tetrahydropalmatrubine (**9**) Obtained from the LC/APCI-MS Data

precursor	callus ^a	alkaloid fraction ^b	selected ions [M + H] ⁺			
			<i>m/z</i> 342 (8)		<i>m/z</i> 342 (9)	
			<i>R</i>	<i>S</i>	<i>R</i>	<i>S</i>
2	A	E-1	25	75	63	37
	A	E-2	36	64	71	29
	B	E-1	38	62	56	44
	B	E-2	12	88	60	40
	C	E-1	46	54	61	39
	C	E-2	33	67	48	52

^a A: *M. cordata*. B: *C. platycarpa*. C: *C. ochotensis* var. *raddeana*. ^b Each fraction is shown in Figure 2.

2,4-dichlorophenoxyacetic acid (1 mg/L), kinetin (0.1 mg/L), yeast extract (0.1%), and agar (1%). The callus tissues were subcultured every 3 or 4 weeks on the same fresh medium at 25 °C in the dark.

S-Corytenchicine (**8**) [$[\alpha]_D -304.8^\circ$ (*c* 0.31, CHCl₃)] is a natural product obtained from *Monanthotaxis fornicata*. Racemic

Table 3. Composition (%) of the Enantiomers of Corytenchicine (**8**) and Tetrahydropalmatrubine (**9**) Obtained from the LC/CD Data

precursor	callus ^a	alkaloid fraction ^b	8		9	
			<i>R</i>	<i>S</i>	<i>R</i>	<i>S</i>
2	A	E-1	31	69	nt	
	A	E-2	35	65	72	28
	B	E-1	24	76	nt	
	B	E-2	2 ^c	98	nt	
	C	E-1	36	64	71	29

^a A: *M. cordata*. B: *C. platycarpa*. C: *C. ochotensis* var. *raddeana*. ^b Each fraction is shown in Figure 2. ^c Shoulder nt: not determined.

tetrahydropapaverine (**1**) was purchased from Sigma Chemical Co.

HPLC Parameters for LC/NMR, LC/MS, and LC/CD. Chromatographic preparations were performed using a Cosmosil 5 C₁₈-AR (4.6 i.d. × 150 mm) reversed-phase column. As a mobile phase (A) 0.1 M NH₄OAc (0.05% TFA, D₂O for LC/NMR) and (B) CH₃CN (0.05% TFA) were used by linear or nonlinear gradient elution. The chiral analytical separation

was carried out on a chiral OJ-RH column (2.0 i.d. × 150 mm, Daicel Chemical Ltd.) at room temperature for the LC/MS and 40 °C for the LC/CD.

LC/APCI-MS Method. LC/APCI-MS (I) for acid-cleavage products of tetrahydropapaverine (**1**) was carried out using a Hitachi M-1000H connected to a Hitachi L-6200 intelligent pump and a Hitachi L-4000 UV detector. APCI-MS (I) conditions: nebulizer and vaporizer temperatures were 330 and 399 °C, respectively. The drift voltage was 40 V. The quasi-molecular ions were monitored in the SIM method. LC was performed on a Cosmosil 5 C₁₈-AR (4.6 i.d. × 150 mm) reversed-phase column. The mobile phase was 0.1 M NH₄OAc (0.05% TFA, A), to which CH₃OH (0.05% TFA, B) was added by a linear gradient: initial 20% of B and 80 min 100% of B. The flow rate was 1 mL/min (detection: 280 nm). LC/APCI-MS/MS was measured on an Applied Biosystems API 3000 Triple Quadrupole mass spectrometer (MS/MS) with a heated nebulizer interface.

Data were collected and processed using Sciex Analyst 1.3 software. Conditions: ion source, APCI; scan type, Q1 scan or product ion scan; source temperature, 400 °C; ion source voltage, 5000 V; nebulizer and curtain gases (nitrogen) 10 and 10, respectively; Q1 scan and product ion scan using IDA method modes were used in MS acquisition method; mass range, 130–430; collision energy, 35–45 V. The mass spectrometer was connected to a Shimadzu LC-10AD_{VP} intelligent pump and a Shimadzu SPD-10A_{VP} UV detector. A nonlinear gradient—initial 20% of B, 25 min 45% of B, 26 min 100% of B—was programmed. The flow rates were 1 and 0.5 mL/min for achiral (Cosmosil 5 C₁₈-AR) and chiral (Chiralcell OJ-RH) chromatography, respectively (detection: 280 nm).

LC-NMR Method. LC-NMR data were acquired using a Varian UNITY-INOVA-500 spectrometer (¹H: 499.83 MHz) equipped with a 60 μL triple-resonance microflow NMR probe. H-1 1D NMR spectra were obtained in stopped-flow mode. Varian WET solvent suppression¹⁶ and related sequences were used to suppress the peaks of CH₃CN, its C-13 satellites, and the residual HOD in D₂O. The WET technique used a series of variable tip-angle solvent-selective radio frequency (rf) pulses, where each selective rf pulse is followed by a dephasing field gradient pulse. FIDs were collected with 32K data points, a spectral width of 9000 Hz, a 3 ms 90° pulse, a 1.82 s acquisition time, and a 0.08 s pulse delay. Typically, 8–392 scans were accumulated (1–13 min). Prior to Fourier transformation, an exponential apodization function was applied to the FID corresponding to a line broadening of 1 Hz. The NOESY spectra were obtained using a WET-NOESY pulse sequence, in which the WET element was incorporated into the 700 ms mixing time. A total of 128 hypercomplex t₁ increments with 16–96 (depending on the sample concentration) transients and 2K data points were acquired with a spectral width in both dimensions of 3500 Hz with an acquisition time of 0.15 s, with total acquisition time of 2–14 h. The data were Gaussian weighted in f₂ and f₁ and zero filled in f₁ to 2K × 2K. The HPLC system consisted of a Varian Pro Star Model-230, solvent delivery system, and Varian Pro Star Model-310 variable-wavelength UV–vis detector. The outlet of the UV detector was connected via a sampling unit (Rheodyne) to the LC-NMR probe. A nonlinear gradient—initial 20% of B, 5 min 30% of B, 15 min 30% of B, and 25 min 100% of B—was programmed. The flow rate was 1 mL/min (detection: 280 nm).

LC/CD Method. Chromatographic separation was performed using a Jasco PU-2080Plus intelligent pump with a column oven (Jasco 860-CO) and a Jasco Browin NT, HSS-2000 data processor, and a Jasco CD-2095Plus CD chiral detector (Hg-Xe lamp), simultaneously monitoring the CD and UV signals at one specific wavelength (range 220–420 nm). A nonlinear gradient—initial 20% of B, 10 min 40% of B, 20 min 40% of B, 30 min 100% of B—was programmed. The flow rate was 0.5 mL/min (detection: 236 nm).

Preparation of Phenolic 1-Benzyltetrahydroisoquinolines 2, 3, 4, and 5. A solution of racemic tetrahydropapaverine hydrochloride (**1**) (Sigma) (500 mg) in concentrated HCl (5 mL) was refluxed for 5.5 h. Hydrochloric acid was evaporated

in vacuo. The residue (330 mg) was dissolved in DMSO (0.5 mL) and was separated by preparative HPLC (a Hitachi L-6250 intelligent pump and a Hitachi L-4000 UV detector), which was performed on a Cosmosil 5 C₁₈-AR (20 i.d. × 250 mm) reversed-phase column. As a mobile phase (A) 0.1 M NH₄OAc (0.05% TFA) and (B) CH₃OH (0.05% TFA) were used by a linear gradient: initial 20% of B and 80 min 100% of B. The flow rate was 6 mL/min (detection: 280 nm). The eluent obtained from the peaks b–e in the LC (Figure 1) was evaporated, and the residue was further purified by HPLC [H₂O (0.05% TFA)–CH₃OH (0.05% TFA)] to give the trifluoroacetates of **2** (11 mg), a mixture of **3** and **4** (26 mg), and **5** (17 mg). The mixture of **3** and **4** was separated by repeated preparative HPLC to afford a small amount of **3** and a mixture of **3** and **4**. **2**: ¹H NMR (CD₃OD, 500 MHz) δ 6.93 (1H, d, *J* = 8.3 Hz, H-5'), 6.80 (1H, s, H-5), 6.78 (1H, d, *J* = 2.0 Hz, H-2'), 6.73 (1H, dd, *J* = 8.3, 2.0 Hz, H-6'), 6.54 (1H, s, H-8), 4.65 (1H, t, *J* = 7.0 Hz, H-1), 3.86 (3H, s, 4'-OCH₃), 3.82 (3H, s, 6-OCH₃), 3.67 (3H, s, 7-OCH₃), 3.53 (1H, m, H-3), 3.33 (2H, m, H-3 and H-9), 3.1–2.99 (3H, m, H-4 and H-9). **3**: ¹H NMR (CD₃OD, 500 MHz) δ 6.84 (1H, d, *J* = 1.5 Hz, H-2'), 6.81 (1H, d, *J* = 8.3 Hz, H-5'), 6.80 (1H, s, H-5), 6.75 (1H, dd, *J* = 8.3, 1.5 Hz, H-6'), 6.56 (1H, s, H-8), 4.68 (1H, t, *J* = 7.5 Hz, H-1), 3.82 (6H, s, 3'- and 6-OCH₃), 3.68 (3H, s, 7-OCH₃), 3.52 (1H, m, H-3), 3.36 (1H, dd, *J* = 14.0, 7.0 Hz, H-9), 3.34 (1H, m, H-3), 3.07 (1H, dd, *J* = 14.0, 8.0 Hz, H-9), 3.07–2.99 (2H, m, H-4). **5**: ¹H NMR (DMSO-*d*₆, 500 MHz) δ 6.89 (1H, d, *J* = 2.0 Hz, H-2'), 6.78 (1H, s, H-5), 6.75 (1H, d, *J* = 8.0 Hz, H-5'), 6.70 (1H, dd, *J* = 8.0, 2.0 Hz, H-6'), 6.62 (1H, s, H-8), 4.57 (1H, t, *J* = 7.0 Hz, H-1), 3.75 (3H, s, 3'-OCH₃), 3.74 (3H, s, 4'-OCH₃), 3.62 (3H, s, 7-OCH₃), 3.36 (1H, m, H-3), 3.26 (1H, dd, *J* = 14.0, 6.5 Hz, H-9), 3.19 (1H, m, H-3), 2.95 (1H, dd, *J* = 14.0, 8.0 Hz, H-9), 2.96–2.84 (2H, m, H-4).

Preparations of Racemic Corytenchine (8), Tetrahydropalmatrubine (9), and Their Enantiomers. To a solution of **2** (50 mg) dissolved in EtOH (6 mL) was added 37% formaldehyde (200 mL). The solution was allowed to stand for one week at room temperature to give a mixture of **8** and **9** (59 mg). The mixture of **8** and **9** (50 mg) was separated by preparative HPLC on a Cosmosil 5 C₁₈-AR (20 i.d. × 250 mm) reversed-phase column (a Hitachi L-6250 intelligent pump and a Hitachi L-4000 UV detector). The mobile phases (A) 0.1 M NH₄OAc (0.05% TFA) and (B) CH₃OH (0.05% TFA) were used for a linear gradient: initial 20% of B and 40 min 100% of B. The flow rate was 6 mL/min (detection: 280 nm). Each eluent obtained from the peaks (*t*_R = 14.46 and 15.95 min) corresponding to **8** and **9** was evaporated, and the residue was further purified by HPLC [H₂O (0.05% TFA)–CH₃OH (0.05% TFA)] to give **8** (13.9 mg) and **9** (34.3 mg) as trifluoroacetates. **8**: ¹H NMR (CD₃OD, 500 MHz) δ 6.94 (1H, s, H-1), 6.82 (1H, s, H-4), 6.77 (1H, s, H-9), 6.75 (1H, s, H-12), 4.55 (1H, brd, *J* = 11 Hz, H-13a), 4.42 (1H, d, *J* = 15.0 Hz, H-8), 4.38 (1H, brd, *J* = 15.0 Hz, H-8), 3.86 (3H, s, 3-OCH₃), 3.85 (3H, s, 10-OCH₃), 3.83 (3H, s, 2-OCH₃), 3.72–3.66 (2H, m, H-6 and H-13), 3.4–3.19 (2H, m, H-5 and H-6), 3.04–2.93 (2H, m, H-5 and H-13); SIMS *m/z* 342 [M + H]⁺ (100), 192 (53); HRSIMS *m/z* 342.1719 (calcd for C₂₀H₂₄O₄N, 342.1704). **9**: ¹H NMR (CD₃OD, 500 MHz) δ 6.95 (1H, s, H-1), 6.94 (1H, d, *J* = 8.3 Hz, H-11), 6.81 (1H, s, H-4), 6.78 (1H, d, *J* = 8.3 Hz, H-12), 4.62 (1H, d, *J* = 16.0 Hz, H-8), 4.47 (1H, brd, *J* = 10 Hz, H-13a), 4.16 (1H, brd, *J* = 16.0 Hz, H-8), 3.86 (3H, s, 10-OCH₃), 3.856 (3H, s, 3-OCH₃), 3.84 (3H, s, 2-OCH₃), 3.75–3.69 (2H, m, H-6 and H-13), 3.33–3.19 (2H, m, H-5 and H-6), 3.03–2.96 (2H, m, H-5 and H-13); SIMS *m/z* 342 [M + H]⁺ (100), 192 (10); HRSIMS *m/z* 342.1715 (calcd for C₂₀H₂₄O₄N, 342.1704). Chiral separation of tetrahydropalmatrubine (**9**) was performed using a chiral OJ-RH reversed-phase column (2.0 i.d. × 150 mm) (a Jasco 880-PU intelligent pump and a Jasco 875-UV detector). As a mobile phase (A) 0.1 M NH₄OAc (0.05% TFA) and (B) CH₃CN (0.05% TFA) were used for nonlinear gradient: initial 20% of B, 10 min 40% of B, and 20 min 40% of B. The flow rate was 0.5 mL/min (detection: 280 nm). Each eluent obtained from the peaks corresponding to *R*-**9** (*t*_R = 16.6 min) and *S*-**9** (*t*_R = 19.2 min) was evaporated, and the residue was

further purified by HPLC [H_2O (0.05% TFA)– CH_3OH (0.05%TFA)] to give *R*-**9** [14.2 mg, $[\alpha]_{\text{D}} +136.4^\circ$ (*c* 0.286, CH_3OH)] and *S*-**9** [13.5 mg, $[\alpha]_{\text{D}} -146.9^\circ$ (*c* 0.715, CH_3OH)] as trifluoroacetates.

Feeding Experiments. Substrates were dissolved in H_2O (2–4 mL) and introduced through a sterile bacterial filter into 100 mL conical flasks containing 40 mL of autoclaved MS medium, identical with that employed in the subculture. Calli (ca. 4–5 g) were transferred to each conical flask and incubated at 25 °C in the dark for an appropriate time (Table 1). Cells and medium were separated and extracted with CH_3OH at 60 °C. Extracts were worked up as described in Figure 2.

References and Notes

- (1) Iwasa, K. In *The Alkaloids*; Cordell G. A., Ed.; Academic Press: New York, 1995; Vol. 46, pp 273–346.
- (2) Iwasa, K.; Nanba, H.; Lee, D.-U.; Kang, S.-I. *Planta Med.* **1997**, *64*, 748–751.
- (3) Iwasa, K.; Nishiyama, Y.; Ichimaru, M.; Moriyasu, M.; Kim, H.-S.; Wataya, Y.; Yamori, T.; Turuo, T.; Lee, D.-U. *Eur. J. Med. Chem.* **1999**, *34*, 1077–1083.
- (4) Iwasa, K.; Moriyasu, M.; Yamori, T.; Turuo, T.; Lee, D.-U.; Wiegrebe, W. *J. Nat. Prod.* **2001**, *64*, 896–898.
- (5) Iwasa, K.; Moriyasu, M.; Tachibana, Y.; Kim, H.-S.; Wataya, Y.; Wiegrebe, W.; Bastow, K. F.; Cosentino, L. M.; Kozuka, M.; Lee, K.-H. *Bioorg. Med. Chem.* **2001**, *9*, 2871–2884.
- (6) Preininger, V. In *The Alkaloids*; Brossi, A., Ed.; Academic Press: New York, 1986; Vol. 29, pp 1–98.
- (7) Zenk, M. H. *Pure Appl. Chem.* **1994**, *66*, 2023–2028.
- (8) Iwasa, K.; Kuribayashi, A.; Sugiura, M.; Moriyasu, M.; Lee, D.-U.; Wiegrebe, W. *Phytochemistry* **2003**, *64*, 1229–1238.
- (9) Hostettmann, K.; Potterat, O.; Wolfender, J.-L. *Pharm. Ind.* **1977**, *59*, 339–347.
- (10) Wolfender, J.-L.; Ndjoko, K.; Hostettmann, K. *Curr. Org. Chem.* **1998**, *2*, 575–596.
- (11) Wolfender, J.-L.; Ndjoko, K.; Hostettmann, K. *Phytochem. Anal.* **2001**, *12*, 2–22.
- (12) Kudo, K.; Ajima, K.; Sakamoto, M.; Saito, M.; Morris, S.; Castiglioni, E. *Chromatography* **1999**, *20*, 59–64.
- (13) Kametani, T.; Ihara, M.; Fukumoto, K.; Yagi, H.; Shimanouchi, H.; Sasada, Y. *Tetrahedron Lett.* **1968**, *40*, 4251–4254.
- (14) Jeffs, P. W. In *The Alkaloids*; Manske, R. H. F., Ed.; Academic Press: New York, 1967; Vol. 9, pp 41–115.
- (15) Lu, S.-T.; Su, T.-L.; Kametani, T.; Ujiie, A.; Ihara, M.; Fukumoto, K. *J. Chem. Soc., Perkin Trans. 1* **1976**, 63–68.
- (16) Smallcombe, S. H.; Patt, S. L.; Keifer, P. A. *J. Magn. Reson. Ser. A* **1995**, *117*, 295–303.

NP0402219